Multipolar ordering in NpO_2 below 25 K

2003 J. Phys.: Condens. Matter 15 S2287

(http://iopscience.iop.org/0953-8984/15/28/370)

INSTITUTE OF PHYSICS PUBLISHING JOURNAL OF PHYSICS: CONDENSED MATTER

J. Phys.: Condens. Matter **15** (2003) S2287–S2296 PII: S0953-8984(03)62921-8

Multipolar ordering in NpO_2 below 25 K

R Caciuffo[1,7], J A Paixão[2], C Detlefs[3], M J Longfield[4], P Santini[5], N Bernhoeft[6], J Rebizant[4] and G H Lander[4]

[1] INFM, Dipartimento di Fisica ed Ingegneria dei Materiali e del Territorio, Università di Ancona, Via Brecce Bianche, I-60131 Ancona, Italy
[2] Departamento de Física, Universidade de Coimbra, P-3004 516 Coimbra, Portugal
[3] European Synchrotron Radiation Facility, BP 220, F-38043 Grenoble, France
[4] European Commission, JRC, Institute for Transuranium Elements, Postfach 2340, D-76125 Karlsruhe, Germany
[5] INFM, Dipartimento di Fisica, Università di Parma, I-43100 Parma, Italy
[6] DRF-MC, CEA-Grenoble, F-38054 Grenoble, France

E-mail: rgc@univpm.it

Received 12 November 2002
Published 4 July 2003
Online at stacks.iop.org/JPhysCM/15/S2287

Abstract

The phase transition at $T_0 = 25$ K in NpO_2 and the single-ion nature of the Np 5f electrons is examined in the light of the results of resonant x-ray scattering experiments at the M_4 Np edge. These experiments exclude usual magnetic dipole ordering at T_0, and provide direct evidence of long-range order of the electric quadrupole moment with Γ_5 symmetry. The phase transition is purely electronic and does not involve either internal or external crystallographic distortions, so the symmetry of the system remains cubic. The primary order parameter (OP) is associated with Γ_4^t magnetic octupoles, ordering in a triple-$\vec{q}$ longitudinal structure defined by the three wavevectors of the $\langle 001 \rangle$ star. Magnetic octupolar order breaks invariance under time reversal and induces the order of electric quadrupoles as the secondary OP. The resulting ground state is a singlet with zero dipole magnetic moment.

1. Introduction

Actinide dioxides are ionic compounds made up of An^{4+} and $2O^{2-}$. At room temperature they all have the fcc crystal structure of CaF_2, with space group *Fm3m*. However, they are simple systems only in appearance. Their physical properties exhibit many fascinating details whose understanding, despite half a century of effort, is still a challenge to theorists and experimentalists. The origin of this complexity essentially lies in the interplay between crystal field (CF), superexchange interactions and electron–phonon coupling. In the case of UO_2, a satisfactory picture is available [1]. The discontinuous phase transition occurring in this

[7] Author to whom any correspondence should be addressed.

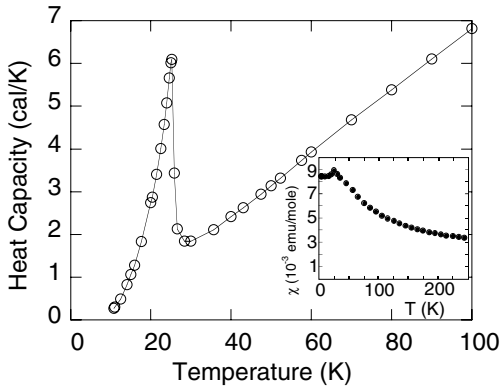

Figure 1. Heat capacity [2] and magnetic susceptibility [3] of NpO_2 as a function of temperature.

compound at $T_N = 30.8$ K is well described as due to the onset of triple-$\vec{q}$, antiferromagnetic (AF) type-I order associated with a triple-$\vec{q}$ distortion of the oxygen cube. The dynamics are also well understood, even though some surprise linked to a strong magnon–phonon coupling could still be hidden. Understanding the behaviour of NpO_2 has proved to be considerably harder.

The first heat capacity measurements for NpO_2 were reported in 1953 [2] and showed a large λ-like anomaly at $T_0 = 25$ K, very similar to that observed earlier for UO_2 at $T_N = 30.8$ K (figure 1). Since Np^{4+} ($5f^3$, $^4I_{9/2}$ in the Russell–Saunders approximation) is a Kramers ion, the CF GS is expected to be magnetic, and the anomaly in the heat capacity was attributed to magnetic order. A maximum at T_0 in the magnetic susceptibility curve corroborated the hypothesis of an ordered low-temperature magnetic phase [3]. However, neither Mößbauer spectroscopy [4] nor neutron diffraction experiments [5–7] have found evidence of magnetic ordering in NpO_2. The upper limit on the ordered magnetic moment set by Mößbauer spectroscopy is $\mu_0 < 0.01\ \mu_B$, to be compared with the effective Curie–Weiss paramagnetic moment of $\sim 3\ \mu_B$. If the magnetic moment is not ordered, the magnetic susceptibility should diverge as the temperature decreases towards zero. On the contrary, the measured susceptibility reaches a constant value of 8.4×10^{-3} emu mol^{-1} at 4 K (figure 1, inset) which implies that the magnetic moment itself becomes negligible below T_0 [8]. A tentative effort to reconcile this fact with the Kramers nature of Np^{4+} ions was made by Solt and Erdös [9], who proposed a model involving a Jahn–Teller (JT) quadrupole-driven monoclinic distortion of the oxygen sublattice and an accidental vanishing of the ordered magnetic moment. The CF potential required in [9] is close to that refined from inelastic neutron scattering (INS) experiments [10], but the model also implies a unidentified anisotropy mechanism forcing the moment to line up along a particular direction, as the three components of $\vec{\mu}$ cannot be simultaneously zero for any particular set of the CF parameters [10]. However, single-crystal diffraction experiments with neutrons [7] and x-rays [11] have found no evidence for a static distortion. A search by neutron diffraction for anharmonic effects showed no observable deformation of either the Np or O restoring potential at low temperature [12], and this also excludes any dynamical distortion model [13]. All available information suggests that the low-temperature GS of NpO_2 preserves the cubic symmetry.

Muon spin relaxation is a sensitive method to detect small moments. When applied to NpO_2, this technique showed oscillations of the backward–forward asymmetry decay below T_0, indicating that the order parameter (OP) of the phase transition sets up a static interstitial

magnetic field and breaks invariance under time reversal [14]. If this signal were due to conventional magnetic dipole order, as in UO_2, it would correspond to a $\mu_0 \approx 0.1\ \mu_B$, a value not compatible with the tiny broadening of the resonance line in Mößbauer spectra. To overcome this contradiction, Santini and Amoretti [15] proposed to describe the phase transition as an ordering of magnetic octupoles, instead of magnetic dipoles. Such an ordering would split the CF ground multiplet, which is known to be a Γ_8 quartet from neutron spectroscopy [16], yet preserving the cubic symmetry. A GS with zero dipole magnetic moment can be obtained for an ordering of either Γ_2 or Γ_5 octupoles. In the first case, the 5f charge density would have cubic symmetry with zero electric quadrupole moments, that would be different from zero in the second case.

New light on the curious phenomenology of NpO_2 was shed recently by resonant x-ray scattering (RXS) experiments performed at the Np M_4 absorption edge [11, 17]. In the following paragraphs we shall describe the techniques employed and the results obtained.

2. Experimental details and results

The experiments were performed on the ID20 beamline of the European Synchrotron Radiation Facility (ESRF) in Grenoble, France, using a 99% σ-polarized incident beam (linear polarization perpendicular to the vertical scattering plane). A flux-grown single crystal of $0.7 \times 0.7 \times 0.2\ mm^3$ in volume (mosaic width 0.01°) was mounted in a closed-cycle refrigerator, equipped with an azimuthal-rotation stage. The exposed face was perpendicular to the [001] axis. Data were taken with photon energies around the Np M_4-edge ($E_{M_4} = 3.845$ keV), using the (111) reflection from a Au mosaic crystal to analyse whether the polarization of the scattered beam was parallel (π) or perpendicular (σ) to the scattering plane (Bragg angle of 43.2° at 3.845 keV; no correction was performed to account for the departure from the ideal 45° orientation). The energy resolution was of about 0.5 eV (full width at half maximum) and the beam flux at 3.845 keV was estimated as 5×10^{11} photons s^{-1}. Here we report results obtained in specular geometry involving scans around reciprocal lattice points of the type $(00L)$.

With a vertical scattering plane and σ incident polarization, the amplitude of magnetic scattering from a given atom at the 3d–5f electric–dipole (E1) threshold is the product of a geometric factor, depending on the polarization of the incident ($\vec{\epsilon}$) and scattered ($\vec{\epsilon'}$) photons, and a linear combination of resonance strength factors, $F_{L=1,M}$,

$$f \propto (\vec{\epsilon} \times \vec{\epsilon'})[F_{1,1} - F_{1,-1}]. \tag{1}$$

Magnetic scattering in the mentioned geometry therefore requires a rotation of the photon polarization, and a difference in the transition probabilities to intermediate states with $M = \pm 1$. This asymmetry can arise because of the net spin polarization of the 5f states, or from a difference between overlap integrals, resonant energy or lifetime for spin-up and spin-down channels [18–20].

RXS can also signal long-range order of anisotropic charge distributions. It is the asphericity of the atomic electron density that generates the anomalous tensor component in the atomic scattering factor. This is the so-called Templeton scattering [21–23] and is observed, for instance, in the case of antiferro-electric order of the quadrupole moments. The scattering amplitude arising from E1 transitions can be described by second-rank tensors $f(\vec{r})$, invariant under the point symmetry of the scattering atom. If $\tilde{f}(\vec{Q})$ is the Fourier transform of $f(\vec{r})$, the scattering amplitude can be written as

$$F(\vec{Q}) = \vec{\epsilon}' \cdot \tilde{f}(\vec{Q}) \cdot \vec{\epsilon}. \tag{2}$$

Below T_0, resonant super-lattice reflections with propagation vector $\langle 001 \rangle$, forbidden within the *Fm3m* space group, have been observed [11]. Figure 2 shows, as an example, the

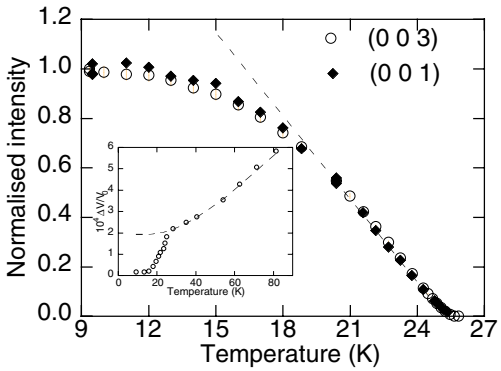

Figure 2. Normalized intensity of the (001) and (003) Bragg peaks as a function of temperature. The straight line is a fit to a power law with a critical exponent $\beta = 0.5$. The inset shows the volume of the cubic unit cell as a function of temperature. The broken curve is the thermal expansion due to anharmonic vibrational effects. Taken from [11].

(This figure is in colour only in the electronic version)

temperature dependence of the intensity of the (001) and (003) Bragg peaks. The reported data are normalized to unity at 10 K, and have been obtained without polarization analysis at 3.845 keV. The phase transition appears continuous, whereas the transition to the AF phase in UO_2 is strongly first order. The line in figure 2 is a fit to a power law giving a critical exponent $\beta = 0.5(1)$.

No diffraction peaks corresponding to a deformation of the oxygen cube have been found. Superstructure reflections are expected for inhomogeneous internal distortions resulting from combinations of normal modes of the oxygen sub-lattice, as observed in UO_2 [24]. We have explored several positions in reciprocal space corresponding to different allowed distortions, with null result. For this experiment, we used a photon energy of 8 keV and a Ge (333) analyser to select the σ–σ polarization channel, where structural Bragg peaks give a contribution. From the statistical error on the background, we estimate an upper limit for extra intensity of the order of $\sim 10^{-8}$ of the fluorite-type charge intensities. This corresponds to an upper limit for the oxygen displacement of about 4×10^{-4}, which effectively excludes inhomogeneous internal distortions. Homogeneous internal distortions, corresponding to normal modes of the oxygen cage and producing only changes in the intensities of fluorine-structure peaks, were excluded by neutron diffraction [12]. A departure from the cubic symmetry, an external distortion, was also checked with null result by following the angular position and width of the (006) lattice reflection. On the other hand, as shown in the inset of figure 2, an anomalous volume contraction of the cubic cell is observed on cooling below T_0 ($\Delta V/V = 1.8(2) \times 10^{-4}$). A similar, but smaller, volume contraction has been observed in UO_2, where a discontinuity $\Delta V/V = 6 \times 10^{-5}$ has been measured at T_N using strain-gauge techniques [25]. This effect can be attributed to magnetoelastic interactions, with the volume contraction proportional to the expectation value of the quadrupolar operators. The results shown in the inset of figure 2 therefore suggest that quadrupolar ordering is established below T_0 in NpO_2.

The integrated intensity of the (003) superlattice peak is shown in figure 3(a) as a function of the photon energy around the M_4 absorption edge of Np. Data were collected at $T = 10$ K, with π polarization of the scattered photon beam, and are corrected for self-absorption. The same energy dependence is shown by the intensity of the σ polarization component of the scattered beam. A resonant behaviour in the σ–σ channel of the structurally forbidden peaks

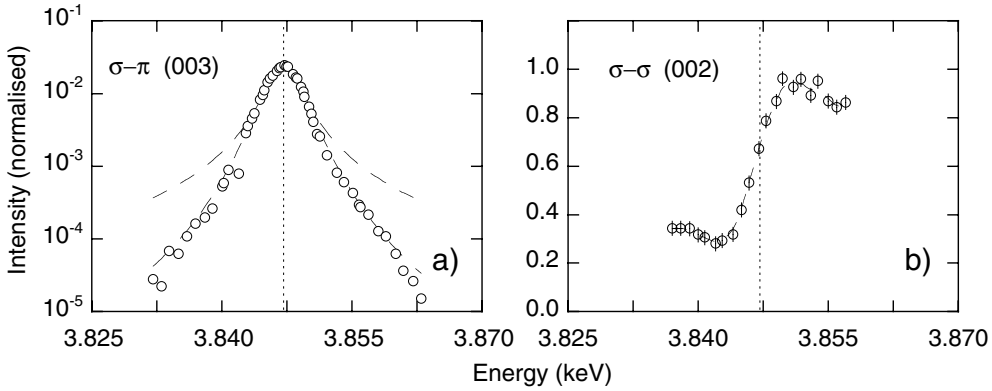

Figure 3. Energy dependence of (a) the (003) superlattice peak intensity at $T = 10$ K in the σ–π channel and (b) the (002) fluorite-type reflection intensity measured with σ final polarization. The (003) σ–π resonance is fitted to a Lorentzian squared line shape. A fit to a Lorentzian is shown by the dotted line for comparison. The vertical dotted line locates the dipole energy threshold at the Np M_4 absorption edge.

indicates that they do not stem from conventional, dipole magnetic order. In that case, in fact, an intensity enhancement occurs only for the σ–π channel. On the other hand, only the variation of absorption across the edge determines the intensity variation of structurally allowed reflections, such as the (002) charge peak. This is shown in panel (b) of figure 3, where the energy dependence of the σ–σ (002) integrated intensity is reported. The inflection point in figure 3(b) identifies the E1, dipole, threshold energy. The fact that the maximum of the resonant (003) peak also occurs at the E1 energy allows us to associate the enhancement of the intensity with a $3d_{3/2} \rightarrow 5f$ transition.

The shape of the resonance, which is fitted in figure 3(a) to a Lorentzian-squared function, is a peculiar result. The intensity enhancement of peaks corresponding to conventional magnetic order has, usually, a simple Lorentzian shape. A Lorentzian squared is expected when the scattering length is given by the difference of two contributions of comparable amplitude, with a splitting of the intermediate state much smaller than the core-hole lifetime.

The results of (003) azimuthal scans performed at $E = 3.846$ keV and $T = 12$ K, for both π and σ final polarization, are reported in figure 4. The intensity of the peak is measured while the sample is rotated around the scattering vector $\vec{Q}$, kept constant at the chosen value. The origin of the azimuthal angle, Ψ, is defined where the a-axis is within the scattering plane. The presence of components in both the $\sigma \rightarrow \pi$ and $\sigma \rightarrow \sigma$ polarization channels, depending on Ψ, is in direct contradiction with the cross-section of E1-magnetic resonant scattering.

3. Triple-$\vec{q}$ antiferro-quadrupolar order

As dipole magnetic order is excluded, the simplest hypothesis is to attribute the origin of the superlattice peaks to the asphericity of the 5f-electron clouds, i.e. to assume an ordered distribution of electric quadrupole moments. To preserve the cubic symmetry, a triple-$\vec{q}$ structure is required, which is obtained when the three elements of the star of $\langle 001 \rangle$ enter the Fourier expansion of the electric quadrupole distribution. Considering Γ_5 quadrupole operators, $P_{ij} = (J_i J_i + J_j J_i)/2$ ($ijk = xyz$ and $\vec{J}$ being the angular momentum operator), the quadrupole moment at a generic Np position r_α is given by

$$\vec{A}(\vec{r}_\alpha) = \Phi(\exp[\mathrm{i}2\pi(y_\alpha + z_\alpha)], \exp[\mathrm{i}2\pi(z_\alpha + x_\alpha)], \exp[\mathrm{i}2\pi(x_\alpha + y_\alpha)]) \qquad (3)$$

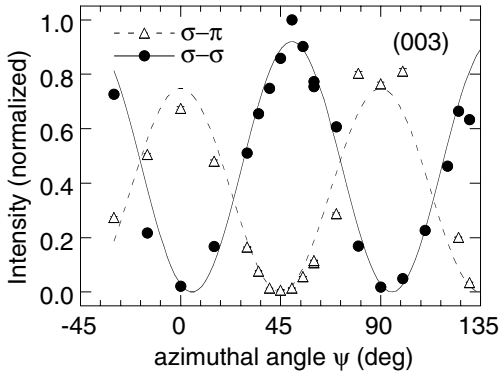

Figure 4. Azimuthal angle dependence of the (003) intensity, at $T = 10$ K, with π and σ final polarization. Curves are calculations based on equation (6).

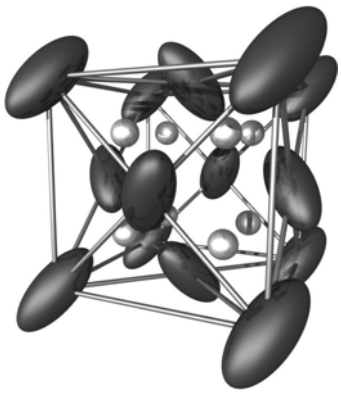

Figure 5. Triple-$\vec{q}$ AF-quadrupolar arrangement of Γ_5 electric quadrupoles in NpO_2. The ellipsoids represent the orientation of the local symmetry axis.

where Φ is the quadrupole OP, assumed to be isotropic. The resulting structure is shown in figure 5, where the ellipsoids represent the orientation of the local symmetry axis at the Np positions. As a consequence of the quadrupole order, the symmetry is lowered from $Fm\bar{3}m$ to $Pn\bar{3}m$. However, with Np ions on 4b and O ions on 2a and 6d Wyckoff positions, the crystallographic structure is indistinguishable from that of the para-quadrupolar phase. The point symmetry at Np site is reduced to D_{3d} but the crystallographic extinction rules remain those of the $Fm\bar{3}m$ space group.

For the given structure and $Q = (00L)$ reflections, the Fourier transform of the second-rank tensor relevant for the calculation of the resonant scattering amplitude is symmetric and can be written as

$$\tilde{f}(\vec{Q}) = 4\tilde{\Phi}\begin{pmatrix} 0 & 1 & 0 \\ 1 & 0 & 0 \\ 0 & 0 & 0 \end{pmatrix} \tag{4}$$

with the resonant pre-factor included in the Fourier transform of the quadrupole OP, $\tilde{\Phi}$. The azimuthal and polarization dependence of the RXS intensity $I(\vec{Q}) = |F(\vec{Q})|^2$ is then easily calculated using equation (2):

$$F(\vec{Q}) = 4\Phi(\epsilon'_x\epsilon_y + \epsilon'_y\epsilon_x) \tag{5}$$

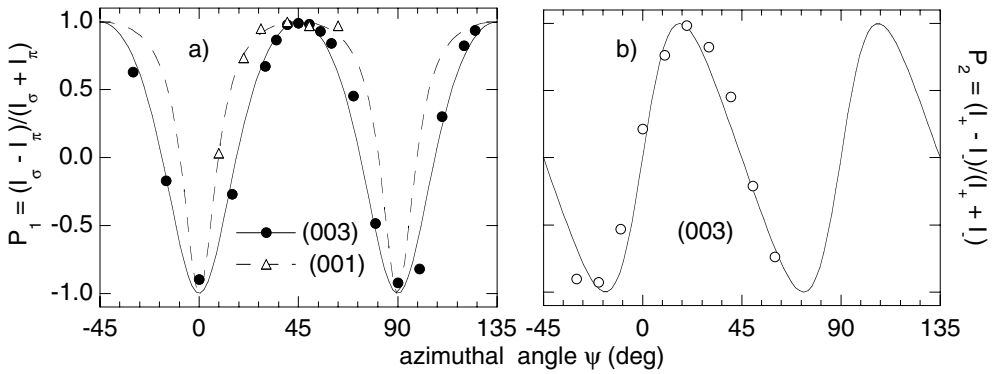

Figure 6. Azimuthal angle dependence of the Stokes parameters P_1 (a) and P_2 (b) of superlattice reflections measured at 10 K with $E = 3.846$ keV. Curves are calculations based on equations (7).

with σ-polarized incident photons, and $\Psi = 0$ where the [100] vector is in the scattering plane; from the above equation one obtains

$$\begin{aligned} F_{\sigma\sigma} &= 4\Phi \sin(2\Psi) \\ F_{\sigma\pi} &= 4\Phi \sin(\theta)\cos(2\Psi). \end{aligned} \tag{6}$$

Intensities calculated with equation (6) for the (003) peak are compared with the experimental results in figure 4. The agreement is more than satisfactory when one considers that the only fitting parameter is a scale factor common to the two set of data. The scale factor is cancelled in the definition of the Stokes parameters P_1 and P_2, that can be directly calculated:

$$\begin{aligned} P_1 &= \frac{I_{\sigma\sigma} - I_{\sigma\pi}}{I_{\sigma\sigma} + I_{\sigma\pi}} = \frac{\sin^2(2\Psi) - \sin^2(\theta)\cos^2(2\Psi)}{1 - \cos^2(\theta)\cos^2(2\Psi)} \\ P_2 &= \frac{|F_{\sigma\sigma} + F_{\sigma\pi}|^2 - |F_{\sigma\sigma} - F_{\sigma\pi}|^2}{|F_{\sigma\sigma} + F_{\sigma\pi}|^2 + |F_{\sigma\sigma} - F_{\sigma\pi}|^2} = \frac{\sin(\theta)\sin(4\Psi)}{1 - \cos^2(\theta)\cos^2(2\Psi)}. \end{aligned} \tag{7}$$

Figure 6 shows the excellent agreement between model predictions and experimental data for the (001) and (003) Bragg peaks.

4. Triple-$\vec{q}$ magnetic-octupole order

The RXS results presented in the previous paragraphs give evidence for electric-quadrupole order below T_0. However, quadrupolar order alone cannot explain the characteristics of the GS. A quadrupole OP Φ was considered in [8–10] (Φ_{xy}) and [13] ($\Phi_{3z^2-r^2}$). The charge distortion detected by our RXS data corresponds rather to quadrupole moments of the form $3z_1^2 - r^2$, where the z_1 axis is parallel to a cube diagonal. In all cases, Φ alone would split the Γ_8 quartet into two magnetic Kramers doublets, and therefore the susceptibility $\chi(T)$ should display Curie–Weiss behaviour as $T \to 0$ (and, eventually, magnetic order would set in), while the observed χ saturates at low T [8]. In addition, μSR experiments [14] show that the OP sets up a magnetic field at the muon stopping site, and therefore the OP has to break time-reversal invariance. This is inconsistent with an electric-quadrupole OP.

The lowest-rank multipolar OP not showing these inconsistencies is a magnetic octupole distinct from the magnetic dipole, i.e. belonging to a representation of the point group different from Γ_4 [15]. In fact, Γ_4 octupoles would always induce a magnetic dipole secondary OP

having the same T dependence. Of course, the opposite is true as well, and in a magnetically ordered material corresponds to nondipolar components of the magnetization density, which can be detected by neutron diffraction at large wavevector transfers. Purely octupolar order corresponds instead to a static magnetization density $M_{ion}(\vec{x})$ around each Np ion which integrates to zero (zero dipole moment), but which is locally nonzero.

Thus, in a cubic CF only four out of seven octupoles are actually distinct from the dipoles. These belong to either the 3D Γ_5 representation or to the 1D Γ_2 representation. Moreover, of the eight possible representations to which the CF GS may belong (Γ_1–Γ_8), only two, i.e. Γ_3 and Γ_8, carry Γ_2 or Γ_5 magnetic-octupole degrees of freedom. Note that in lower symmetries the situation is even worse, for instance in tetragonal symmetry only two octupoles are distinct from dipoles, and in most compounds, moreover, these remaining purely octupolar degrees of freedom are quenched by the CF. Thus, even if superexchange or the RKKY mechanism are likely to provide sizeable octupolar couplings in a number of compounds, and these couplings might exceed dipolar couplings in a fraction of these compounds, only very few of them would possess the characteristics needed for a purely octupolar phase transition to occur, i.e. high enough symmetry and the right CF GS. For instance, such a phase transition would be impossible in UO_2 because of its Γ_5 CF GS. In contrast, the Γ_8 CF GS of NpO_2 carries both Γ_5 and Γ_2 octupole degrees of freedom.

A Γ_2 OP ($\propto J_x J_y J_z$) is consistent with most properties of NpO_2 [15], but it cannot explain the RXS results, as it does not carry an electric quadrupole moment and the $\sigma \rightarrow \sigma$ signal would vanish [26]. Γ_5 octupolar operators are given by combinations of $O_x = J_x(J_y^2 - J_z^2)$, $O_y = J_y(J_z^2 - J_x^2)$ and $O_z = J_z(J_x^2 - J_y^2)$ operators, properly symmetrized. The little cogroup of the ordering wavevector is D_{4h}. Γ_5 decomposes into the tetragonal representations $\Gamma_4^{(t)}$ (1D) and $\Gamma_5^{(t)}$ (2D), which identify two possible type-I orders, a 'longitudinal' one and a 'transverse' one. For a single- or double-$\vec{q}$ structure, both types of OP are inconsistent with the observed quenching of dipoles and with the present RXS results. There is just one single type of order which can explain all observations, and this is a triple-$\vec{q}$ longitudinal structure, in which the $\Gamma_4^{(t)}$ OPs associated with the three wavevectors of the star of $\vec{q}$ have the same amplitude, ρ.

The simplest conceivable mean-field (MF) Hamiltonian for each of the four sublattices s is given by

$$H = W\left(x\frac{O_4}{F(4)} + (1-|x|)\frac{O_6}{F(6)}\right) - \lambda O[\vec{n}(s)]\langle O[\vec{n}(s)]\rangle(T). \tag{8}$$

We consider the $^4I_{9/2}$ Russel–Saunders ground manifold only, thus J-$mixing$ is neglected. The first part represents the cubic CF, in the usual notation [27], with $-1 \leqslant x \leqslant 1$. The values of the CF parameters x and W are derived by scaling those of UO_2, $x_{UO_2} = 0.9$, $W_{UO_2} = 4.3$ meV $\rightarrow x_{NpO_2} = -0.75$, $W_{NpO_2} = -1.74$ meV. With these values the first excited CF state is a Γ_8 quartet, 49 meV above a Γ_8 quartet GS, in agreement with INS results. The second term is an MF octupolar interaction, where $\vec{n}(s)$ represents one of the four inequivalent $\langle 111\rangle$ directions, $O[\vec{n}(s)] = \sum_{l=x,y,z} O_l n_l(s)$, and $\langle O[\vec{n}(s)]\rangle(T)$ is the self-consistent average value of $O[\vec{n}(s)]$, which does not depend on s. λ is left as a free parameter. It is proportional to the Fourier transform of ion–ion octupole couplings at $\vec{q} = \langle 100\rangle$. The interaction produces a second-order phase transition towards a state with $\langle O[\vec{n}(s)]\rangle \neq 0$, at a transition temperature T_0 given by the MF relation $\chi_{oct}^{-1}(T_0) = \lambda$, with $\chi_{oct}(T)$ the static ionic octupolar susceptibility.

The MF term lowers the symmetry of the Np Hamiltonian from O_h to D_{3d} and splits the Γ_8-quartet CF ground state into two singlets, Γ_5 and Γ_6, and one doublet, Γ_4, of D_{3d}. Γ_5 and Γ_6 are complex-conjugate representations, which are degenerate for a time-reversal invariant Hamiltonian, whereas their degeneracy is lifted by the time-odd OP. By choosing the value of λ

which reproduces the observed T_0, the level sequence at $T = 0$ is found to be singlet–doublet–singlet. The GS has vanishing dipole moment and the susceptibility saturates for $T \to 0$, as observed [8]. These properties do not depend on the details of the CF Hamiltonian (i.e. on the precise value of the CF parameter x or whether J-mixing is taken into account).

This octupolar OP induces the observed triple-$\vec{q}$ structure of Γ_5 quadrupoles as the secondary OP, with an amplitude $\propto \rho^2$ in MF near T_0. The charge density is distorted along $\vec{n}(s)$. This can be quantified by the average value of the quadrupolar operator along $\vec{n}(s)$,

$$\Phi(\vec{n}(s)) = \alpha\langle r^2\rangle[3(\vec{n}(s)\cdot\vec{J})^2 - J(J+1)] \tag{9}$$

where $\langle r^2\rangle$ is the average squared radius of 5f electrons, and $\alpha = -6.43 \times 10^{-3}$ is the second-order Stevens coefficient, which relates the physical quadrupolar moment to its operator equivalent. Φ is negative in the ordered phase, indicating that the charge distribution is oblate along $\vec{n}(s)$. This quadrupolar secondary OP is the quantity observed in the RXS experiment. The secondary character of the quadrupole moment is consistent with the large value observed for the critical exponent β ($\sim$0.5 [11]). Given that superexchange interactions are short range, this value of β would be unusually large if the quantity accessed by RXS were a primary OP, whereas a larger value (by a factor of two in MF) is expected for a secondary OP.

5. Conclusions

RXS experiments in NpO_2 are interpreted as evidence for the development of electric quadrupole order below the transition temperature $T_0 = 25$ K. Quadrupolar ordering is assumed to be driven by a primary magnetic octupole OP. The model we propose excludes a lattice distortion or a shift of the oxygen positions. The octupolar order breaks time-reversal symmetry and thus allows the occurrence of interstitial magnetic fields as evidenced by μSR [14, 15]. In addition, the reduction of the local symmetry at the Np site leads to an electric field gradient along the $\langle 111\rangle$ directions. This explains the line broadening observed below T_0 in Mößbauer spectroscopy [13, 28]. The sample dependence of the line broadening can be easily understood by noting that if the local symmetry of the high-T phase is lower than cubic due to a defect, a magnetic-dipole secondary OP would generally exist locally. Its effect on the nuclear levels would superpose with the quadrupole effect of the nondefective regions. The overall splitting of the Γ_8 GS is expected to be of the order of 10 meV, compatible with the value deduced by INS [29]. However, a second energy scale, outside the range explored by INS, is also predicted. Available heat capacity data for NpO_2 do not extend below 11 K, so that the relevant temperature range has not yet been explored. However, the entropy in excess of the estimated lattice entropy from 11 K up to the phase transition is 1.70 cal K^{-1} mol^{-1}, significantly smaller than the expected spin-only value ($R \ln 4 = 2.75$ cal K^{-1} mol^{-1}) [2]. This could be an indication of anomalies in the heat capacity below 11 K, corresponding to further loss of magnetic entropy. Heat capacity measurements to verify this point have been planned.

Acknowledgments

We thank the ESRF and the beamline staff on ID20 for help with the experiments. Discussions with G Amoretti and R Waldstedt are gratefully acknowledged.

References

[1] Caciuffo R *et al* 1999 *Phys. Rev.* B **59** 13892
[2] Osborne D W and Westrum E F 1953 *J. Chem. Phys.* **21** 1884
[3] Ross J W and Lam D J 1967 *J. Appl. Phys.* **38** 1451
[4] Dunlap B D *et al* 1968 *J. Phys. Chem. Solids* **29** 1365

[5] Cox D E and Frazer B C 1967 *J. Phys. Chem. Solids* **28** 1649
[6] Heaton L, Müller M H and Williams J M 1967 *J. Phys. Chem. Solids* **28** 1651
[7] Boeuf A *et al* 1983 *Phys. Status Solidi* **79** K1
[8] Erdös P *et al* 1980 *Physica* B **102** 164
[9] Solt G and Erdös P 1980 *J. Magn. Magn. Mater.* **15–18** 57
[10] Amoretti G *et al* 1992 *J. Phys.: Condens. Matter* **4** 3459
[11] Mannix D *et al* 1999 *Phys. Rev.* B **60** 15187
[12] Caciuffo R *et al* 1987 *Solid State Commun.* **64** 149
[13] Friedt J M, Litterst F J and Rebizant J 1985 *Phys. Rev.* B **32** 257
[14] Kopmann W *et al* 1998 *J. Alloys Compounds* **271–273** 463
[15] Santini P and Amoretti G 2000 *Phys. Rev. Lett.* **85** 2188
Santini P and Amoretti G 2000 *Phys. Rev. Lett.* **85** 5481 (eratum)
[16] Fournier J M *et al* 1991 *Phys. Rev.* B **43** 1142
[17] Paixão J A *et al* 2002 *Phys. Rev. Lett.* **89** 187202
[18] Hill J P and McMorrow D F 1996 *Acta Crystallogr.* A **52** 236
[19] Blume M 1985 *J. Appl. Phys.* **57** 3615
[20] Blume M and Gibbs D 1988 *Phys. Rev.* B **37** 1779
[21] Templeton D H and Templeton L K 1985 *Acta Crystallogr.* A **41** 133
[22] Dmitrienko V E 1983 *Acta Crystallogr.* A **39** 29
[23] Dmitrienko V E 1984 *Acta Crystallogr.* A **40** 89
[24] Faber J and Lander G H 1976 *Phys. Rev.* B **14** 1151
[25] Brandt O G and Walker C T 1967 *Phys. Rev. Lett.* **18** 11
[26] Lovesey S W 1996 *J. Phys.: Condens. Matter* **8** 11009
[27] Lea K R, Leask M G M and Wolf W P 1962 *J. Phys. Chem. Solids* **23** 1381
[28] Masaki N M *et al* 2000 *Physica* B **281/282** 256
[29] Caciuffo R *et al* 1991 *Solid State Commun.* **69** 197